Available online at www.sciencedirect.com
SCIENCE DIRECT
Catalysis Today 115 (2006) 222–227
CATALYSIS TODAY
www.elsevier.com/locate/cattod

Methanol synthesis from CO_2-rich syngas over a ZrO_2 doped CuZnO catalyst

Cheng Yang [a], Zhongyi Ma [a], Ning Zhao [a], Wei Wei [a], Tiandou Hu [b], Yuhan Sun [a,*]

[a] State Key Laboratory of Coal Conversion, Institute of Coal Chemistry, Chinese Academy of Sciences, Taiyuan 030001, PR China
[b] Beijing Synchrotron Radiation Facility, Institute of High Energy Physics, Chinese Academy of Sciences, Beijing 100039, PR China

Available online 4 May 2006

Abstract

ZrO_2-doped CuZnO catalyst prepared by successive-precipitation method was investigated by ICP-AES, BET, TEM, XRD, EXAFS, H_2-TPR and CO/CO_2 hydrogenation. The active phase of copper in CuZnO catalyst prepared by co-precipitation method was well-crystallized. The presence of ZrO_2 led to a high copper dispersion, which was distinctive from CuZnO. Though the activity for carbon monoxide hydrogenation was little lower than that of CuZnO catalyst, ZrO_2-doped CuZnO catalyst showed much higher activity and selectivity towards methanol synthesis from carbon dioxide hydrogenation. Moreover, ZrO_2-doped CuZnO catalyst showed high performance for methanol synthesis from CO_2-rich syngas.

Keywords: CuZnO catalyst; ZrO_2-doped; CO/CO_2 hydrogenation; CO_2-rich syngas; Methanol synthesis

1. Introduction

Methanol is considered an alternative energy source, a medium for the storage and transportation of hydrogen and a starting feedstock for many chemicals as well. Commercially, methanol is produced from natural gas or coal via syngas, mainly containing CO and H_2 along with a small amount of CO_2, which has been developed by ICI, Lurgi, Topsoe and MGC etc. over the last century. The potential use of CO_2, the most important greenhouse gas, as an alternative feedstock replacing CO in the methanol production has received attention as an effective way of CO_2 utilization. Under proper conditions, methanol made from atmospheric CO_2 by its reaction with hydrogen is regarded as the ''most economic way'' after oil and gas [1].

Methanol is currently produced from syngas using a ternary Cu–Zn–Al oxide catalyst at 5.0–10.0 MPa and 473–523 K. However, the ternary catalyst that was active for CO-rich feed stock was not so active for the CO_2-rich sources [2,3]. Although the mechanism of methanol synthesis from CO/CO_2 hydrogenation is still controversial, the kinetic experiments, conducted with isotope-labelled CO and spectroscopy [4–6], have demonstrated that under industrial conditions, methanol was produced by hydrogenation of CO_2, with CO merely providing a source of CO_2 and acting as a reducing agent by scavenging surface oxygen. Moreover, it was reported that CO_2 kept the copper surface partially oxidized or prevented an over-reduction of the ZnO component [7–9]. The water formed as a by-product, from both methanol synthesis and the RWGS side reaction, also had an inhibitory effect on the active copper metal during the reaction [10,11]. Of further interest was that a mixture with a proper proportion of CO_2 and CO not only increased the yield of methanol but also decreased the apparent activation energy of the reaction [12]. At present, the key to methanol synthesis is to develop the most efficient catalyst for both CO and CO_2 hydrogenation. Within above context there have been claims that the performance of the catalyst could be improved. The majority of the catalysts still contain Cu and Zn as the main components together with different modifiers as well as using different preparation methods [2,13–17].

Cu/ZrO_2 was well known as an active catalyst for CO/CO_2 hydrogenation [18]. Nitta et al. [19] reported that the proper addition of certain amounts of ZnO to the Cu/ZrO_2 catalyst could greatly enhance its activity. Liaw and Chen [20] obtained ultrafine Cu/ZnO-based catalysts using a reduction method in which the dispersion and stability of copper could be improved by doping Cr, Zr and Th. In other words, for the catalyst to possess higher activity, selectivity and long life, it was

* Corresponding author. Tel.: +86 351 2023638; fax: +86 351 4041153.
E-mail address: yhsun@sxicc.ac.cn (Y. Sun).

0920-5861/$ – see front matter
doi:10.1016/j.cattod.2006.02.077

important to obtain a catalyst with large surface area, fine particle size and a high dispersion of active sites.

In the present work, a novel ZrO_2 doped CuZnO catalyst was developed for methanol synthesis from CO/CO_2 hydrogenation. Structural properties of catalysts were characterized by ICP-AES, BET, TEM, XRD, EXAFS and H_2-TPR techniques.

2. Experimental

2.1. Catalysts preparation

Zr–Cu/ZnO catalyst was prepared by successive-precipitation method using the respective metal nitrates and different alkali salts. The precursor of ZnO was prepared by adding an aqueous solution of $Zn(NO_3)_2$ and an aqueous solution of Na_2CO_3 simultaneously at 343 K and a constant pH of 9 in a well-stirred thermo-stated container. The suspension was vigorously stirred and kept at the desired pH, then the aqueous solution of $Cu(NO_3)_2$ and $ZrO(NO_3)_2$ was co-precipitated with $NH_3{\cdot}H_2O$ under the same conditions. The precipitates were aged at 343 K for 4 h. Afterward the precipitates were washed thoroughly with distilled water and dried at 393 K for 12 h. After calcined at 673 K in air for 4 h, a ZrO_2-doped CuZnO catalyst (denoted as Zr–Cu/ZnO) was obtained. A reference CuZnO catalyst with a nominal composition of Cu:Zn = 60:40 (wt.%) was prepared by co-precipitation of the corresponding metal nitrates with Na_2CO_3, followed by aging, washing and drying as described above.

2.2. Characterization methods

The overall chemical compositions were measured using inductively coupled plasma with atomic emission spectroscopy (ICP-AES).

The surface area of the catalysts was measured at 77 K by nitrogen adsorption using a BET apparatus (ASAP 2000), and pore size distribution was estimated from the adsorption branch of the isotherm by the method of Horvath and Kawazoe [21].

Transmission electron micrographs (TEM) experiments were carried out using a H-9000NAR at 400 kV. The samples for micrograph image were prepared by placing the catalysts in ethanol and sonicating for 30 min, then one drop of solution was placed on a 300 mesh copper grid.

X-ray powder (XRD) was performed with a Rigaku diffractometer using Ni-filtered Cu Kα radiation. Patterns were recorded from 15° to 75° (2θ) at 40 kV and 40 mA.

X-ray adsorption spectra around the Cu K-adsorption edge were obtained using the beamline of 4W1B at Beijing Synchrotron Radiation Facility (BSRF). The storage ring was operated at 2.2 GeV with a typical current of 50 mA. The fixed-exit Si (1 1 1) flat double crystals were used as monochromator. The extended X-ray absorption fine structure (EXAFS) data were processed with the National Synchrotron Radiation Laboratory analysis programs (NSRLXAFS).

Temperature program reduction (TPR) was carried out in a U-tube quartz reactor with hydrogen–argon mixture (containing 5 vol.% of hydrogen) as the reductive gas. The samples (50 mg) were flushed with an argon flow of 50 $cm^3\ min^{-1}$ at 393 K to remove water and then reduced in a flow of H_2 + Ar at a rate of 10 K min^{-1} with a programmable temperature controller. Hydrogen consumption was monitored by a thermal conductivity detector (TCD) attached to a gas chromatograph (GC-950). The effluent gas was passed through a cold trap placed before TCD in order to remove water from the exit stream of the reactor.

2.3. Catalytic activity test

CO/CO_2 hydrogenation tests were carried out using a stainless steel fixed-bed reactor, which contained 1.0 ml catalyst. All catalysts were reduced in H_2 (5% in N_2) flow at 533 K and atmospheric pressure for 6 h before syngas exposure. The reaction was conducted at 5.0 MPa overall pressure with a mixture of CO and/or CO_2 and H_2 (GHSV = 4000 h^{-1}). The steady-state activity measurements were taken after at least 24 h on the stream. Shimazu-8A GC was used to analyze the products. H_2, CO, CH_4 and CO_2 were determined by thermal conductivity detector (TCD) equipped with a TDX-101 column. The water and methanol in liquids were also detected by TCD with a GDX-401 column.

3. Results and discussion

Industrial CuZn-based catalysts are commonly prepared by co-precipitation method using the corresponding metal nitrates with aqueous solution of Na_2CO_3. As listed in Table 1, the real metal content of Cu and Zn in the prepared CuZnO catalyst was 42.9 and 26.6 wt.%, approximately with the atomic ratio of 6:4. For Zr–Cu/ZnO catalyst, the proportion of Cu to Zn was about 1:1, containing 13.5 wt.% of Zr as well. The BET surface area of Zr–Cu/ZnO was 62.2 $m^2\ g^{-1}$ with the mean pore radius and pore volume of 10.4 nm and 0.16 $cm^3\ g^{-1}$, respectively. Obviously, Zr–Cu/ZnO had larger BET surface area than CuZnO. Transmission electron micrographs of the catalysts were shown in Fig. 1. The images revealed that the particle size of CuZnO was about 30 nm, while that of Zr–Cu/ZnO was distributed between 10 and 12 nm. These data suggested that Zr–Cu/ZnO catalyst existed in fine particles, which showed distinctive surface physical properties from CuZnO.

The XRD patterns of CuZnO and Zr–Cu/ZnO catalyst were shown in Fig. 2. The sample of CuZnO presented the obvious lines due to CuO and ZnO, illustrating the presence of well-crystallized CuO and ZnO. But no reflections of CuO were detected in Zr–Cu/ZnO catalyst, i.e. the active phase could be highly dispersed. However, the sharper XRD peaks were observed for ZnO in Zr–Cu/ZnO due to the separate formation of its precursor.

Table 1
The textural parameters and metal composition of the catalysts

Catalyst	S_{BET} ($m^2\ g^{-1}$)	V_P ($cm^3\ g^{-1}$)	r_P (nm)	Metal content (wt.%)		
				Cu	Zn	Zr
CuZnO	48.6	0.14	11.4	42.9	26.6	–
Zr–Cu/ZnO	62.2	0.16	10.4	33.1	32.3	13.5

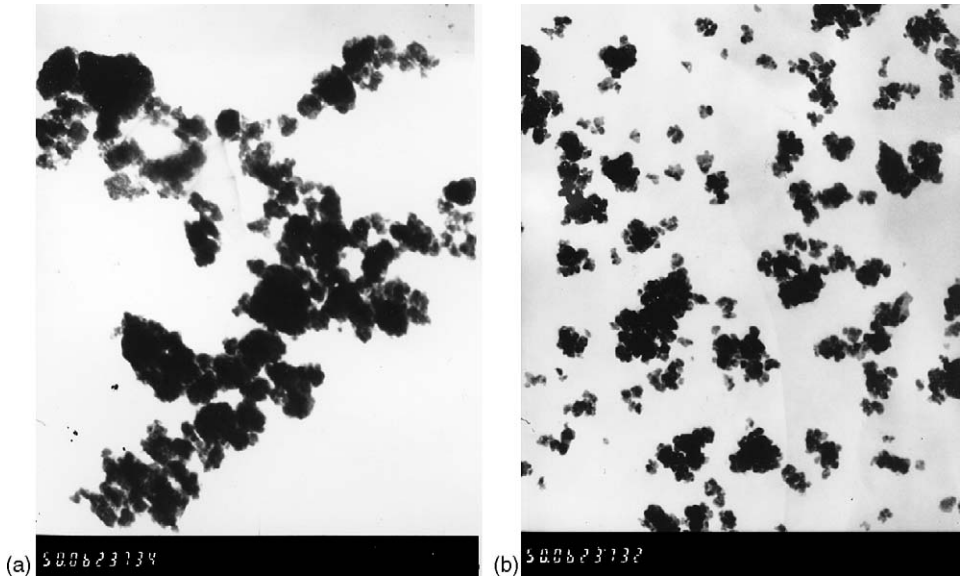

Fig. 1. TEM images of the catalysts: (a) CuZnO; (b) Zr–Cu/ZnO.

Extended X-ray absorption fine structure provided more obvious differences of CuO crystals between the two catalysts. Fig. 3 showed the partial radial distribution function (RDFs) obtained by Fourier transforms of $\kappa^3\chi(\kappa)$ ($\Delta\kappa$ = 3.0–11.5 Å). The $\Delta\kappa$ values were restricted to be relatively narrow, because the Hf L_3-edge (9561 eV) of HfO_2 (presented as an impurity in the zirconia) severely hampered extraction of Cu K-edge oscillations at higher κ values. A total of 4.0 nearest oxygen was found for each copper site at an average distance of 0.195 nm on the bulk CuO and these results were in good agreement with the conclusion of crystal analysis, which indicated that the fixed error in our experimentation and data analysis was very low. The RDF for the two catalysts were significantly different from that of CuO or $Cu(OH)_2$ [22], suggesting the formation of a copper species in a distinct local structure. The clear absence of Cu–Cu bonding at about 3.2 Å (uncorrected for phase shifts) in Zr–Cu/ZnO catalyst indicated that the Cu^{2+} species were highly dispersed, while a peak due to Cu–Cu bonding emerged at 3.4 Å for CuZnO, implying the formation of CuO clusters. The introduction of ZrO_2 had obviously influenced the CuO coordination surroundings. The structural parameters, as derived from an EXAFS analysis, were summarized in Table 2. The lower copper coordination number for Zr–Cu/ZnO than for copper model compounds revealed that the copper species existed in much smaller crystallites and exhibited an amorphous-like or less well-ordered structure feature.

Table 2
Fitting results of CuO EXAFS for Cu–O band

Sample	Shell	Coordination number	Shell radius (nm)	Debye–Waller factors ($\times10^{-4}$ nm^2)
CuO	Cu–O	4.00	0.195	–
CuZnO	Cu–O	3.99	0.197	0.22
Zr–Cu/ZnO	Cu–O	3.59	2.00	1.79

Note: Fitting range in κ-space: 2.0–10.0 Å^{-1} with the weight of κ^3.

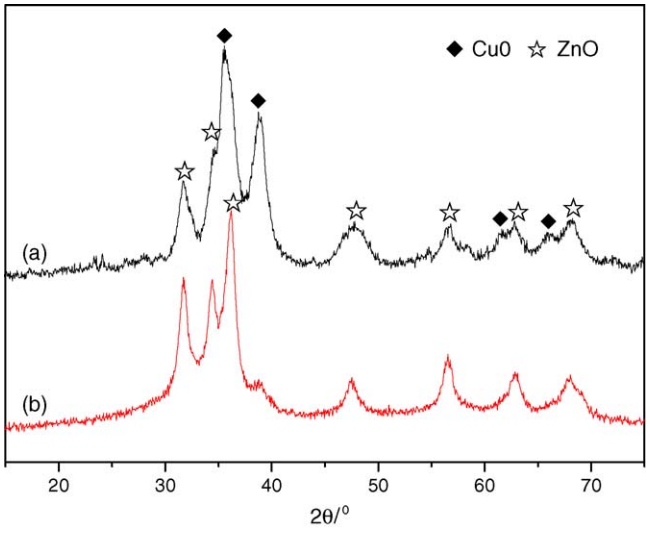

Fig. 2. XRD patterns of the catalysts: (a) CuZnO; (b) Zr–Cu/ZnO.

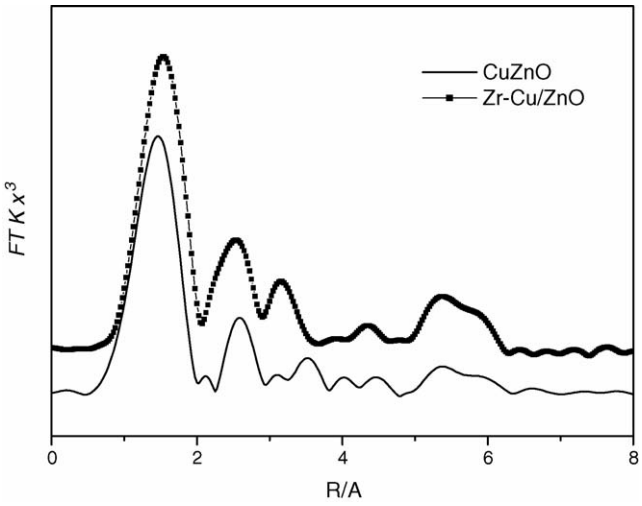

Fig. 3. Radial distribution functions obtained by Fourier transformed of the EXAFS date at the Cu K-edge of the catalysts.

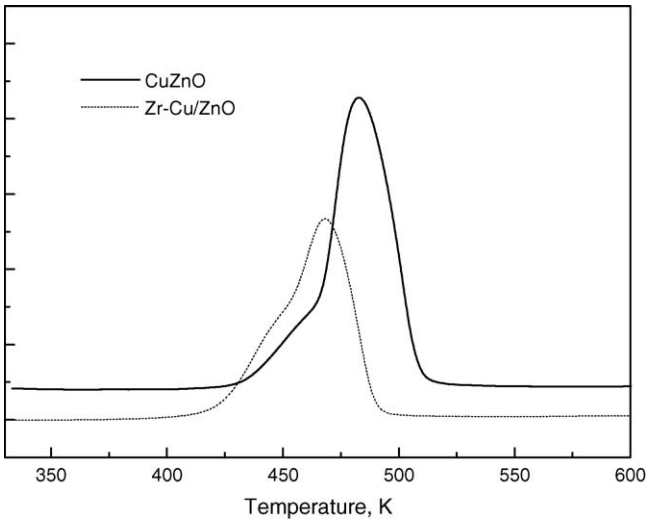

Fig. 4. TPR profiles of the catalysts.

Compared to CuZnO, the copper coordination number for Zr–Cu/ZnO decreased and the distance of Cu–O increased, and the high Debye–Waller factors associated with this shell also indicated that the copper in Zr–Cu/ZnO was present in great disorder. Therefore, the interaction of copper with other components in Zr–Cu/ZnO was stronger than that in CuZnO.

The TPR curves of the two catalysts were illustrated in Fig. 4. CuZnO presented two peaks of hydrogen consumption, corresponding to the reduction of highly dispersed or isolated copper species (at low temperature) and bulk CuO species (at high temperature), respectively [23–25]. The higher area of the peak at high temperature than that at low temperature was indicative of well-crystallized CuO species. Otherwise, the reduction peaks on Zr–Cu/ZnO catalyst were obviously shifted to lower temperatures due to highly dispersed copper species.

CuZnO-based catalyst, especially for the ternary catalyst Cu–Zn–Al, showed high activity and selectivity towards methanol synthesis from CO hydrogenation under mild reaction conditions [2,3]. The CO conversion and methanol yield for the CuZnO and Zr–Cu/ZnO catalysts were displayed as a function of reaction temperature in Fig. 5(A) and (B). Apparently, CuZnO catalyst showed higher activity than Zr–Cu/ZnO at low temperatures. The CO conversion and methanol yield for CuZnO reached maximum of 48% and 0.82 g ml^{-1} h^{-1}, respectively, at about 513 K. It was noted that the CO conversion for Zr–Cu/ZnO catalyst was almost equal to that for CuZnO when the reaction temperature was above 523 K, and the maximum was prolonged to 533 K.

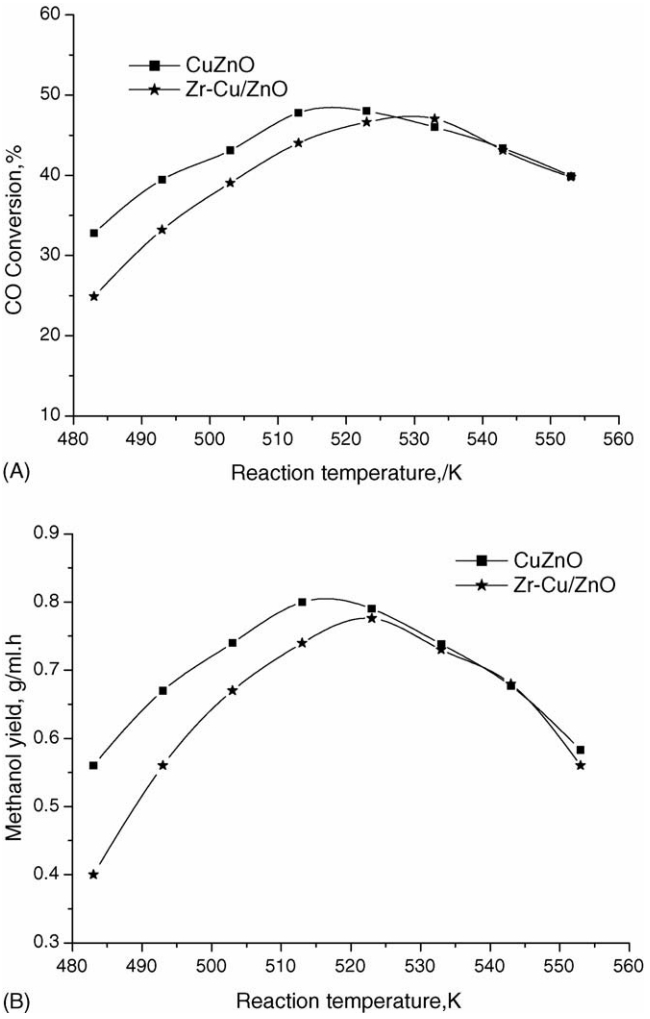

Fig. 5. Catalytic performances of the catalysts for methanol synthesis from CO hydrogenation: (A) CuZnO; (B) Zr–Cu/ZnO. Reaction conditions: P = 5.0 Mpa, GHSV = 4000 h^{-1}, H_2:CO (molar) = 2:1.

In the reaction of CO_2 and H_2, methanol was produced by CO_2 hydrogenation and CO was simultaneously formed by the reverse water–gas shift (RWGS) reaction. The results derived from the catalytic tests were summarized in Table 3. Unlike the

Table 3
The activity and selectivity of the catalyst for methanol synthesis from CO_2 hydrogenation

Catalyst	Reaction temperature (K)	CO_2 conversion (%)	Selectivity (C-mol.%)			MeOH yield (g ml^{-1} h^{-1})
			CO	MeOH	CH_4	
CuZnO	483	9.67	44.82	55.18	0.00	0.08
	503	13.61	49.60	49.08	0.42	0.12
	523	16.03	50.42	47.53	2.05	0.14
	543	20.47	57.74	40.12	2.14	0.14
Zr-Cu/ZnO	483	17.31	44.71	55.29	0.00	0.13
	503	23.46	41.12	58.88	0.00	0.19
	523	26.41	39.55	60.45	0.01	0.22
	543	27.91	48.88	51.12	0.08	0.19

Reaction conditions: P = 5.0 Mpa, GHSV = 4000 h^{-1}, H_2:CO_2 (molar) = 3:1.

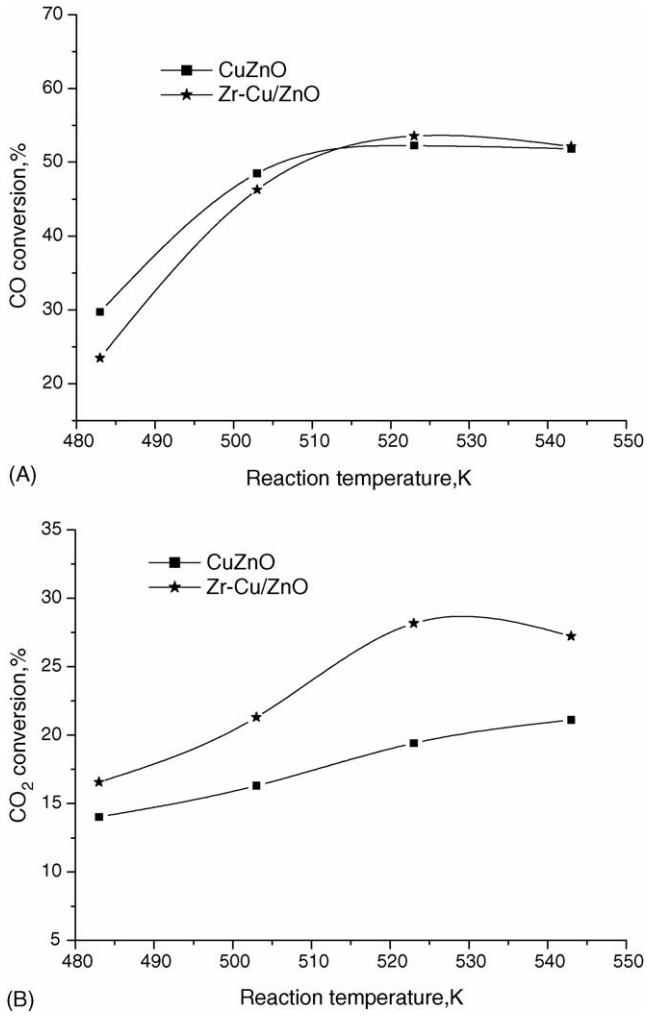

Fig. 6. Catalytic activities of the catalysts for methanol synthesis from CO_2-rich syngas: (A) CuZnO; (B) Zr–Cu/ZnO. Reaction conditions: $P = 5.0$ Mpa, GHSV = 4000 h^{-1}, H_2:CO:CO_2 (molar) = 4:1:1.

catalytic performance for CO conversion, Zr–Cu/ZnO catalyst showed high performance for methanol synthesis from CO_2 hydrogenation. Both CO_2 conversion and methanol selectivity for Zr–Cu/ZnO were higher than that for CuZnO. The CO_2 conversion was found to increase with the rise of reaction temperature. But the methanol selectivity in the C-containing products decreased at high temperatures with the production of a small amount of methane. The methanol yield for Zr–Cu/ZnO catalyst reached maximum of 0.22 g ml^{-1} h^{-1} with the selectivity of 60.45% at about 523 K.

For the mixture of CO and CO_2 reacted with hydrogen over the catalysts, it was interesting to find that both CO and CO_2 conversion was higher compared with the single carbon source (CO or CO_2) at the same temperature and pressure, especially on Zr–Cu/ZnO catalyst. Fig. 6 showed the CO and CO_2 conversion as a function of reaction temperature. Zr–Cu/ZnO almost had the equal CO conversion to CuZnO in all temperatures studied, but much higher CO_2 conversion than CuZnO. Moreover, Zr–Cu/ZnO catalyst showed a high stability after running 1000 h (see Fig. 7). The CO and CO_2 conversion at 523 K was about 55% and 28%, respectively, and the

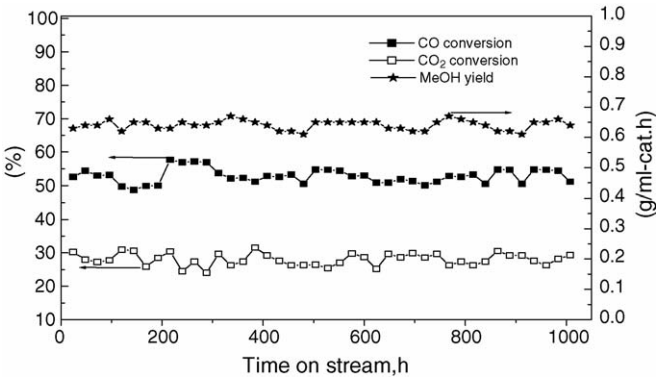

Fig. 7. Stability test of the Zr–Zn/CuO catalyst for 1000 h. Reaction conditions: $T = 523$ K, $P = 5.0$ Mpa, GHSV = 4000 h^{-1}, H_2:CO:CO_2 (molar) = 4:1:1.

methanol yield was about 0.65 g ml^{-1} h^{-1}. No other C-containing products were detected, except for a small trace of methane.

4. Summary

ZrO_2-doped CuZnO catalyst possessed distinctive physic-chemical properties from that of CuZnO. The active copper species were highly dispersed in ZrO_2-doped CuZnO catalyst, while that in CuZnO catalyst were well-crystallized. The interaction of copper with other components in Zr–Cu/ZnO catalyst was stronger than that in CuZnO. Therefore, ZrO_2-doped CuZnO catalyst showed high activity and high selectivity towards both CO and CO_2 hydrogenation, especially for CO_2 hydrogenation.

Acknowledgement

The financial support from the National Nature Science Foundation (Grant no. 20590363) is gratefully acknowledged.

References

[1] G.A. Olah, Catal. Lett. 93 (2004) 1.
[2] M. Saito, T. Fujitani, M. Takeuchi, T. Watanabe, Appl. Catal. 138 (1996) 331.
[3] T. Inui, H. Hara, T. Takeguchi, J.B. Kim, Catal. Today 36 (1997) 25.
[4] G.C. Chinchen, P.J. Denny, D.G. Parker, M.S. Spencer, Appl. Catal. 30 (1987) 333.
[5] M. Bowker, R.A. Hadden, H. Houghton, J.N.K. Hyland, K.C. Waugh, J. Catal. 109 (1988) 263.
[6] J. Weigel, R.A. Koeppel, A. Baiker, A. Wokaun, Langmuir 12 (1996) 5319.
[7] B. Denise, R.P.A. Sneeden, B. Beguin, O. Cherifi, Appl. Catal. 30 (1987) 353.
[8] D.S. King, R.M. Nix, J. Catal. 160 (1996) 76.
[9] J.S. Lee, K.H. Lee, S.Y. Lee, Y.G. Kim, J. Catal. 144 (1993) 414.
[10] K. Fujimoto, Y. Yu, Second Int. Conf. Sillover (1993) 393.
[11] T. Inui, T. Takeguchi, Catal. Today 10 (1991) 95.
[12] X.M. Liu, G.Q. Lu, Z.F. Yan, J. Beltramini, Ind. Eng. Chem. Res. 42 (2003) 6518.
[13] I.M. Cabrera, M.L. Granados, J.L. Fierro, Catal. Lett. 79 (2002) 1.
[14] J.Y. Liu, J.L. Shi, D.H. He, Q.M. Zhu, Appl. Catal. 218 (2001) 113.
[15] Y. Tanaka, C. Kawamura, A. Ueno, K. Takeuchi, Y. Sugi, Appl. Catal. 8 (1983) 325.

[16] J. Toyir, P.R. Piscina, J.L.G. Fierro, N. Homs, Appl. Catal. 29 (2001) 207.
[17] M. Fujiwara, H. Ando, M. Tanaka, Y. Souma, Bull. Chem. Soc. Jpn. 67 (1994) 546.
[18] Y.H. Sun, P.A. Sermon, J. Chem. Soc. Chem. Commun. 16 (1993) 1242.
[19] Y. Nitta, O. Suwata, Y. Okamoto, Catal Lett. 26 (1994) 345.
[20] B.J. Liaw, Y.Z. Chen, Appl. Catal. 206 (2001) 245.
[21] G. Horvath, K. Kawazoe, J. Chem. Eng. Jpn. 16 (1983) 470.
[22] S.F. Chen, G.E. Brown, G.A. Parks, Am. Mineral 85 (2000) 118.
[23] T.M. Yurieva, T.P. Minyukova, React. Kinet. Catal. Lett. 29 (1985) 55.
[24] R.X. Zhou, T.M. Yu, X.Y. Jiang, X.M. Zheng, Appl. Surf. Sci. 148 (1999) 263.
[25] M. Shimokawabe, H. Asakawa, N. Takezawa, Appl. Catal. 59 (1990) 45.